Earth and Planetary Science Letters 394 (2014) 20–29

Contents lists available at ScienceDirect

Earth and Planetary Science Letters

www.elsevier.com/locate/epsl

Assessing influences on speleothem dead carbon variability over the Holocene: Implications for speleothem-based radiocarbon calibration

Alexandra L. Noronha [a,*], Kathleen R. Johnson [a], Chaoyong Hu [b], Jiaoyang Ruan [b,1], John R. Southon [a], Julie E. Ferguson [a]

[a] Department of Earth System Science, University of California, Irvine, CA 92697, USA
[b] State Key Laboratory of Biogeology and Environmental Geology, China University of Geosciences, Wuhan, 430074, PR China

ARTICLE INFO

Article history:
Received 30 August 2013
Received in revised form 26 February 2014
Accepted 9 March 2014
Available online xxxx
Editor: J. Lynch-Stieglitz

Keywords:
radiocarbon
Holocene
speleothem

ABSTRACT

Recently, it has been shown that U–Th dated speleothems may provide a valuable archive of atmospheric radiocarbon (^{14}C), but the reliability of these records is dependent upon the stability of the dead carbon proportion (DCP) derived from the soil and bedrock. In order to assess climatic influences on speleothem DCP, we have investigated DCP variability over the Holocene interval where atmospheric ^{14}C is well known based on dendrochronologically dated tree rings by conducting ^{14}C measurements on a U–Th dated stalagmite (HS4) from Heshang Cave, Hubei Province, China (30°27′N, 110°25′E; 294 m) spanning 0.5–9.6 ka. We investigated climatic controls on DCP, and found that DCP in HS4 has an average value over the Holocene of 10.3 ± 1.5%, with an average age offset from atmospheric radiocarbon of 875 ± 130 years, and displays a response to both precipitation increases and decreases. HS4 DCP increases during the wetter mid-Holocene interval (~5.5–7.1 ka), likely reflecting a shift to more closed-system dissolution in response to increased soil moisture. DCP decreases during the 8.2 ka event, a time period of dry conditions at Heshang Cave, though the lower amplitude of this shift indicates that DCP may be less sensitive to dry events. Speleothems are potentially valuable archives of atmospheric radiocarbon, especially in older portions of the ^{14}C calibration curve where knowledge of atmospheric ^{14}C is limited, however minor climatic influences on DCP could introduce uncertainties of several hundred years to calibrated ages.

1. Introduction

1.1. Calibration of atmospheric radiocarbon

In order to study the causes and effects of past changes in Earth's climate, precise and accurate chronologies and chronometers are key. Many paleoclimate proxy records rely on measurements of the concentration of radiocarbon (^{14}C) in calcite ($CaCO_3$) or organic matter for construction of their calendar age chronologies. However, radiocarbon-based geochronology, which is theoretically possible to at least 50 ka, is complicated by changing atmospheric concentrations of ^{14}C, which are controlled by: (1) non-constant ^{14}C production rates in the upper atmosphere, which vary with geomagnetic field intensity and solar variations over a wide-range of timescales (Bard, 1998), and (2) changes in carbon cycling which redistributes carbon, including ^{14}C, between ocean, atmosphere, and biosphere reservoirs. In order to use ^{14}C as a chronometer, and investigate changes in carbon cycling, the ^{14}C timescale must be calibrated by reconstruction of records of atmospheric ^{14}C tied to robust independent chronologies.

Tree ring records of ^{14}C with calendar ages derived from dendrochronology are considered the most robust records of atmospheric ^{14}C because they directly incorporate atmospheric CO_2 during photosynthesis and have a high-resolution independent chronology. Tree ring records from central and northern Europe are the basis of the most recent IntCal13 radiocarbon calibration curve to 13.9 ka (Reimer et al., 2013). Before this point, regional climate conditions were less hospitable to trees, and the tree ring records are no longer the basis of ^{14}C calibration curves, although there are some floating tree ring chronologies covering earlier intervals (e.g. Turney et al., 2007; Muscheler et al., 2008; Kromer et al., 2004; Hua et al., 2009; Hogg et al., 2013).

* Corresponding author. Tel.: +1 949 824 3674.
E-mail address: anoronha@uci.edu (A.L. Noronha).
[1] Present address: Laboratoire des Sciences du Climat et de l'Environnement (LSCE), CNRS/CEA/UVSQ, L'Orme des Merisiers, 91191 Gif-sur-Yvette Cedex, France.

http://dx.doi.org/10.1016/j.epsl.2014.03.015
0012-821X/

The only true non-tree ring record of atmospheric ^{14}C extending beyond 13.9 ka is a record from Lake Suigetsu, Japan, which is based on macrofossils paired with a varve counting chronology (Kitagawa and van der Plicht, 1998a, 1998b, 2000; Staff et al., 2010; Bronk Ramsey et al., 2012) and covers the interval 0–52.8 ka. The Lake Suigetsu record presented by Kitagawa and van der Plicht (1998a, 1998b, 2000) showed significant divergence from other atmospheric radiocarbon reconstructions prior to ~25 ka, which was found to be due to errors in the calendar chronology because of incomplete core retrieval during sampling (Staff et al., 2010). A new set of overlapping cores was taken and a new high-resolution record with an improved chronology has been constructed, though the record displays large scatter in the ^{14}C ages in the interval >28 ka due to small sample sizes, as well as large uncertainty in the layer-counting age model (Bronk Ramsey et al., 2012). Nonetheless, the Lake Suigetsu ^{14}C record provides a valuable "backbone" for the atmospheric ^{14}C record, which is refined by a variety of other ^{14}C records.

In the absence of true atmospheric records, the majority of calibration efforts have been focused on marine sediment records with a constant correction applied to account for the marine reservoir effect – the offset between the concentration of ^{14}C in the ocean and the atmosphere. The use of marine records for calibration of terrestrial radiocarbon dates is complicated by the potential for climatically driven variations in marine reservoir age. It is well known that large and rapid changes in climate occurred during the deglacial period, which were likely associated with changes in the Atlantic Meridional Overturning Circulation (McManus et al., 2004; Vellinga and Wood, 2002). These climatic changes were accompanied by large variations in surface ocean ^{14}C (Broecker and Barker, 2007; Hughen et al., 2000), consistent with the idea that they involved major shifts in the carbon cycle, which would have had large impacts on marine reservoir ages. Despite this complication, the agreement between these reservoir corrected marine records and the Lake Suigetsu record is very good to ~28 ka. Before 28 ka the divergence between records increases (Reimer et al., 2013), as does the variance in the Lake Suigetsu record (Bronk Ramsey et al., 2012), with differences between records on the order of thousands of years, leading to high uncertainty in the atmospheric ^{14}C record in the earlier intervals.

1.2. Speleothem-based records of atmospheric radiocarbon

Recently, there has been interest in using speleothems to create records for radiocarbon calibration, in part because they have many features which may make them valuable sources of records which resolve the calibration curve in older intervals (e.g. Beck et al., 2001; Weyhenmeyer et al., 2003; Dorale et al., 2008; McDermott et al., 2008; Hoffmann et al., 2010; Southon et al., 2012). Speleothems hold some key advantages over floating tree rings, varved chronologies, and marine records: (1) They can be precisely and absolutely dated using U–Th methods (Richards and Dorale, 2003); (2) Their fast growth rates, highly resolvable stratigraphy, and excellent preservation allow for often continuous high-resolution ^{14}C measurement over the entire ^{14}C dating range; (3) they are widely used for paleoclimate reconstruction (Fairchild et al., 2006) so access to numerous U–Th dated samples is possible and will allow for replication of records and direct comparison with climate proxy data. There are, however, several complicating factors affecting speleothem-based radiocarbon calibrations stemming from the way that speleothems are formed.

Formation of speleothem calcite is driven by CO_2 degassing of cave drip water that has accumulated carbon from the soil and bedrock. Meteoric waters equilibrate with soil CO_2 to form carbonic acid, which drives carbonate dissolution as drip water percolates through the limestone cave host bedrock. Consequently, ^{14}C in speleothem calcite is offset from contemporaneous atmospheric ^{14}C because a proportion of speleothem carbon comes from old soil organic matter (SOM) and radiocarbon-free "dead carbon" from the bedrock. To date, the offset between speleothem ^{14}C and contemporaneous atmospheric ^{14}C has been referred to in a variety of different ways across the literature, often using the same acronym to refer to different metrics, which has been a source of some confusion. In this manuscript we will refer to the dead carbon proportion (DCP) as a percentage as defined by Genty and Massault (1997), but we also refer to the DCP as a "correction" or "offset" with units of ^{14}C years.

Hendy (1971) considered two end member scenarios under which dissolution of carbonate bedrock can occur: open and closed system dissolution. In open-system dissolution, the solution dissolving the bedrock is continually in contact with soil CO_2, which leads to speleothem $\Delta^{14}C$ compositions dominated by a soil CO_2 signature, as isotopic equilibrium with soil C and the dissolved inorganic carbon (DIC) pool is maintained during dissolution. In closed system dissolution, dissolution of the bedrock takes place in isolation from soil CO_2, leading to $\Delta^{14}C$ compositions shifted towards a bedrock ^{14}C isotope signature. Therefore, completely open-system dissolution, where soil CO_2 ^{14}C values are identical to atmospheric values would lead to an apparent DCP = 0%, whereas a completely closed-system dissolution wherein one mole of carbonate is required to neutralize one mole of dissolved CO_2 would lead to a theoretical DCP = 50%. However, soil gas $^{14}CO_2$ is rarely equal to atmospheric $^{14}CO_2$, because soil CO_2 is a mixture of atmospheric CO_2, root respiration, and CO_2 from decomposition of aged SOM, leading to the potential for a DCP > 50%, and making a DCP = 0% unlikely. In natural systems, carbonate dissolution usually falls somewhere between the two end member scenarios, with average DCP around $15 \pm 5\%$ (Genty et al., 1999). Despite the potential for variable DCP to complicate speleothem-based reconstructions of atmospheric ^{14}C, speleothem radiocarbon records have been used to provide valuable constraints on the calibration curve during intervals where true atmospheric ^{14}C data is limited (Beck et al., 2001; Hoffmann et al., 2010; Southon et al., 2012).

The speleothem-based records of atmospheric ^{14}C that have been included in IntCal13 are a record spanning 10.6–26.8 ka from Hulu Cave, China (Southon et al., 2012), and a record spanning 11.1–44.1 from the Bahamas (Beck et al., 2001; Hoffmann et al., 2010). These records were constructed using a trench-and-wall sampling technique, where ^{14}C measurements on intact chips of calcite from the walls are interleaved with U–Th measurements on powder from drilled trenches, resulting in a robust and well-constrained calendar chronology for the ^{14}C record. The record from Hulu Cave, based on speleothem H82, has a very low and stable DCP of $5.4 \pm 0.7\%$ (450 ± 50), calculated from the period of overlap between H82 with the master tree ring records spanning 10.7–12.6 ka, which covers the Younger Dryas/Holocene transition – a period of rapid climate change which is likely to have altered cave hydrology (Southon et al., 2012). The Bahamas speleothem record based on GB-89-24-1 spanning 11–45 ka was initially published in Beck et al. (2001) and showed extremely large variations in ^{14}C in the interval 41–44 ka. These variations were found to be an analytical artifact, and a new sampling of GB-89-24-1 covering 41–44 ka as well as a new record based on speleothem GB-89-25-3 spanning 28–44 ka and 11–15 ka to establish the DCP, was constructed by Hoffmann et al. (2010). GB-89-25-3 has a high DCP of $22.7 \pm 5.9\%$ (2075 ± 540), while GB-89-24-1 has a slightly lower DCP of $16.5 \pm 4.7\%$ (1450 ± 470).

There has been some hesitation in using speleothems for ^{14}C calibration, because of the potential for undetected variations in DCP, as well as the large variations in DCP seen in the Bahamas speleothem records. However, even with this additional

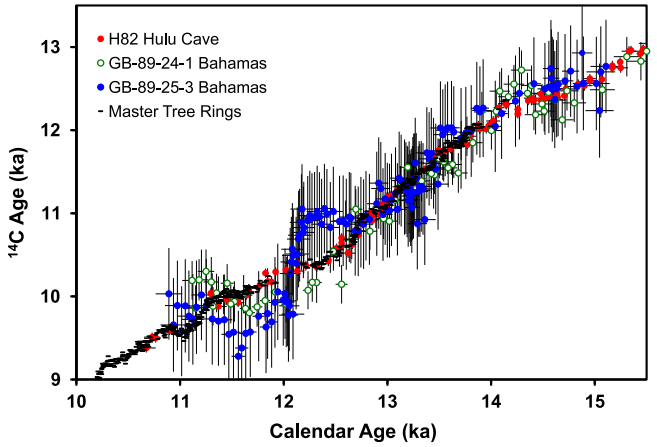

Fig. 1. Comparison of period of overlap between existing speleothem-based reconstructions of atmospheric ^{14}C H82 Hulu Cave (filled red circles), GB-89-24-1 Bahamas speleothem (open green circles), and GB-89-25-3 Bahamas speleothem (filled blue circles) and tree ring records of atmospheric ^{14}C included in IntCal13 (black dashes). (For interpretation of the references to color in this figure legend, the reader is referred to the web version of this article.)

uncertainty, the existing speleothem records of ^{14}C have been instrumental in improving our understanding of the history of the carbon cycle through identifying past changes in ocean circulation, and marine reservoir age, and therefore improving the ^{14}C calibration curve. Comparison between the Cariaco Basin record and both the Hulu Cave speleothem and Bahamas speleothem ^{14}C records confirmed that the marine reservoir age in Cariaco Basin varied significantly during Heinrich Stadial I (Southon et al., 2012), which resulted in the removal of the Cariaco Basin ^{14}C data during Heinrich Stadial I from IntCal13 (Reimer et al., 2013). Additionally, while the new Lake Suigetsu core has an improved varve counting chronology, complications inherent to varve counting based chronologies still limit the certainty of the calendar chronology, especially in older sections. To address this, the drift in the varve chronology was corrected for by comparison between the Lake Suigetsu record and the U–Th based calendar chronology of Hulu Cave H82 and Bahamas GB-89-25-3 speleothem records (Bronk Ramsey et al., 2012), which resulted in major reductions in the 1σ error of the Lake Suigetsu calendar chronology, ranging from a factor of $\sim$2 at 13 ka to at least a factor of 10 at $>$30 ka. The combination of true atmospheric ^{14}C measurements from Lake Suigetsu with robust absolute U–Th based calendar chronology from speleothems has resulted in significant improvement in the calibration curve.

Speleothem records of ^{14}C have proven to be valuable for improving the calibration curve, but to be able to fully take advantage of speleothems as records of atmospheric ^{14}C, improved understanding of the controls on dead carbon incorporation in speleothems must be developed. Reconstructions of ^{14}C in speleothems over the interval where atmospheric ^{14}C is well known from the tree ring record allows for precise constraint on DCP variability and for investigation of the controls on variability in DCP. The Bahamas and Hulu ^{14}C records included in IntCal13 (Southon et al., 2012; Beck et al., 2001; Hoffmann et al., 2010) have very short periods of overlap with the tree ring records (Fig. 1), of only 2.8 ka in GB-89-24-1, 3.1 ka in GB-89-25-3, and 3.2 ka in H82, which severely limits knowledge of the extent of variability of DCP in these records. To study the variation of DCP in speleothem records over a wide range of climatic conditions and over a range of timescales, we have created a stalagmite-based record of Holocene ^{14}C, as the Holocene represents the interval where atmospheric ^{14}C is best known based on dendrochronologically dated trees. This record, based on a Holocene stalagmite referred to as HS4 from Heshang Cave in the Hubei Province of China, is particularly well-suited for this study as it lies in the East Asian Summer Monsoon (EASM) region, a location which has likely experienced large changes in precipitation in response to changing Northern Hemisphere summer insolation (Wang et al., 2008; Morrill et al., 2003; Hu et al., 2008) and abrupt events linked to high-latitudes (Liu et al., 2013). Furthermore, as the HS4 stalagmite has been the subject of extensive paleoclimate research (Johnson et al., 2006; Hu et al., 2008; Liu et al., 2013) and Heshang Cave is the site of a long-term modern calibration study (Hu et al., 2008), robust paleoclimate records are available for comparison with the ^{14}C record. In this paper, we present a new speleothem-based atmospheric ^{14}C record spanning 0.5–9.6 ka based on a total of 84^{14}C measurements made on HS4 with a calendar age model based on U–Th measurements from Hu et al. (2008) and Liu et al. (2013). In addition, to investigate the DCP response to abrupt climate events, we present high-resolution ^{14}C measurements over the 8.2 ka event, a time period characterized by very dry conditions at the cave site (Liu et al., 2013).

2. Study location and methods

Heshang Cave is located in the Hubei Provence of China (30.44°N, 110.42°E), $\sim$100 km west of the city of Yichang in the middle reaches of the Yangtze Valley. The cave is 250 m long, roughly horizontal, well ventilated, and overlain with 400 m of Cambrian dolomite. HS4 is a 2.5 m long annually-banded stalagmite that was actively forming when it was collected from Heshang Cave in 2001. HS4 has previously been measured for δ^{18}O and δ^{13}C at high resolution and an age model was constructed using 21 U–Th measurements and layer-counting (Hu et al., 2008). The stalagmite has a high mean growth rate of 0.28 mm/yr.

The stalagmite was cut in half parallel to the growth axis and the surface was polished to reveal laminations consisting of sub-mm scale light and dark couplets, which have been shown to be annual (Hu et al., 2008). HS4 calcite is milky, opaque, and porous, with a fabric dominantly characterized as open columnar using the terminology of Frisia and Borsato (2010). Fifty-four samples for ^{14}C analysis were taken as intact wafers of calcite using a "moat-and-spall" technique, whereby a small trench is drilled around the desired sample region using a 0.5 mm dental drill and the solid wafer is then snapped off at its base. Similar sampling methods have been employed in this study and previous studies (e.g. Beck et al., 2001; Hoffmann et al., 2010; Southon et al., 2012) because of concern that contamination of sample material by atmospheric CO_2 may occur, as shifts in isotopic values have been observed in some carbonate samples collected as powder (e.g. Gill et al., 1995). 21 wafer samples were taken from the same depths as the original 21 U–Th dates and an additional 33 were interspersed along the HS4 growth axis to give an average spacing of $\sim$1 sample every 4 cm. Wafers were subsequently crushed into smaller pieces to achieve the desired mass of carbon for measurements – typically 12–14 mg of calcite for AMS ^{14}C measurements.

A recent study by Liu et al. (2013) of the 8.2 ka event in Heshang HS4 indicated a sharp decrease in precipitation over Heshang Cave at that time based on δ^{18}O, Mg/Ca, and annual layer thickness evidence. To investigate how abrupt changes in precipitation affect DCP, an additional 30 samples ranging from 3–7 mg were drilled from this interval at 100 µm resolution with a New Wave Research micromill and measured for ^{14}C. At this high resolution samples must be drilled as powder, but the good agreement between these powder samples and the samples drilled as wafers suggests that there was no atmospheric contamination of these samples.

Carbonate samples for ^{14}C measurements drilled as chunks were pretreated with a 30% leach by reaction with a measured volume of weak HCl to dissolve 30% of the sample mass while sam-

ples drilled with powder were only leached 10%. All carbonate was subsequently hydrolyzed in 85% H_3PO_4. Samples were graphitized by iron catalyzed hydrogen reduction following standard protocols, and geologic calcite samples were used as procedural blanks. All radiocarbon measurements were made at University of California Irvine on a NEC Compact (1.5 SDH) AMS system, using six aliquots of Oxalic Acid I as the normalizing standard. Each mg-sized carbon sample was measured multiple times (typically 8–15 runs) over a 24 h period.

Due to the aforementioned disparities in terminology used in the literature to describe the offset between speleothem calcite and contemporaneous atmospheric ^{14}C, we undertake a detailed explanation of the metric we use in this paper, in hopes that perhaps a standard can be set in the literature. In this manuscript the term referred to as the DCP is simply the percentage of old ^{14}C-free "dead carbon" incorporated in the speleothem at the time of formation. The percentage is calculated via the procedure of Genty and Massault (1997):

$$DCP = \left[1 - \left(\frac{a^{14}C_{init}}{a^{14}C_{atm.init.}}\right)\right]100\% \quad (1)$$

where $a^{14}C_{init}$, the initial activity of the calcite is:

$$a^{14}C_{init} = \frac{a^{14}C_{meas}}{e^{\lambda t}} \quad (2)$$

and the atmospheric ^{14}C activity at the time the calcite precipitated, $a^{14}C_{atm.init.}$, is obtained from the ^{14}C calibration curve at the calendar age, λ is the decay constant of ^{14}C, using a 5730 a half life, t is the calendar age of the sample in years, and $a^{14}C_{meas}$ is the ^{14}C concentration measured in the stalagmite. All $a^{14}C$ values are in units of percent modern carbon (pMC). The error in DCP is calculated from the error in the calibration curve, the error in the stalagmite ^{14}C measurement, and the calendar chronology by:

$$\sigma_{DCP} = \left[\left(\frac{a^{14}C_{init}}{a^{14}C_{atm.init.}}\right)\sqrt{\left(\frac{\sigma_{a^{14}C_{init}}}{a^{14}C_{init}}\right)^2 + \left(\frac{\sigma_{a^{14}C_{atm.init.}}}{a^{14}C_{atm.init.}}\right)^2}\right]100\% \quad (3)$$

where the error on the initial activity of the calcite ($a^{14}C_{init}$) is:

$$\sigma_{a^{14}C_{init}} = a^{14}C_{init}\sqrt{\left(\frac{\sigma_{a^{14}C_{meas}}}{a^{14}C_{meas}}\right)^2 + (\lambda\sigma_t)^2} \quad (4)$$

When referring to the age offset in ^{14}C years that results from incorporation of dead carbon, we refer to the DCP "correction" or "offset", which is a simple difference between the measured speleothem ^{14}C and the contemporaneous atmospheric ^{14}C. The error is found by propagating the uncertainty in both the calibration curve and the measured value. In these calculations, because the calibration curve has 5-year resolution over the interval defined by the tree rings in practice the atmospheric ^{14}C age used is that of the nearest IntCal point.

U–Th ages published by Hu et al. (2008) and Liu et al. (2013) are the basis of the calendar age model for HS4. Following the methods of Liu et al. (2013), the age depth model derived from the 9 U–Th dates covering the 8.2 ka event has been refined by the precise annual layer-counting floating age model for the 8.2 ka event using the OxCal Bayesian software (Bronk Ramsey, 2008). The OxCal analysis of the U–Th dates for the 8.2 ka event interval was repeated in this study on the 9 U–Th dates with the addition of the U–Th date from Hu et al. (2008) from 238 cm depth, because of its proximity to the high-resolution U–Th dates and smaller uncertainty relative to the nine high-resolution U–Th dates from Liu et al. (2013). The resulting Bayesian OxCal ages are shown in Table 1. The age model for the HS4 Holocene ^{14}C record was created

Table 1
OxCal Bayesian ages.

Distance from top (cm)	Bayes max (yrs BP)	Bayes min (yrs BP)	Bayes age 1σ error (yrs BP)
228	8024	7844	7934 ± 45
229	8084	7875	7979.5 ± 52
230.1	8147	7909	8028 ± 60
231	8209	7945	8077 ± 66
232	8266	7984	8125 ± 71
233	8320	8025	8172.5 ± 74
234	8373	8066	8219.5 ± 77
235	8432	8117	8274.5 ± 79
235.9	8498	8166	8332 ± 83
236.8	8643	8245	8444 ± 100

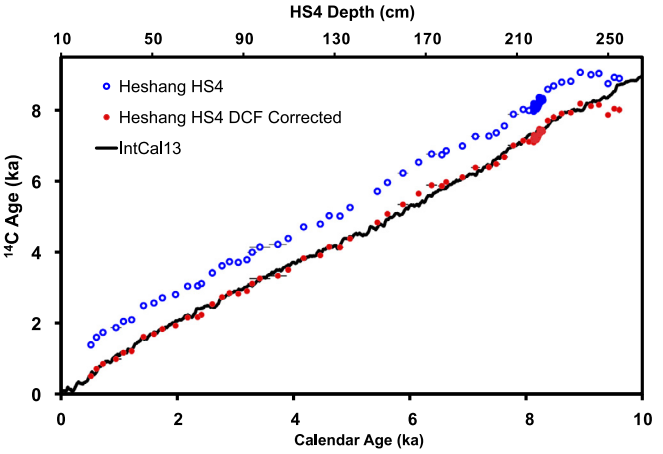

Fig. 2. Comparison of the HS4 ^{14}C record (open blue circles) and the DCF corrected HS4 ^{14}C record (filled red circles) with IntCal13. (For interpretation of the references to color in this figure legend, the reader is referred to the web version of this article.)

using the 10 Bayesian OxCal ages and the remaining 20 U–Th dates from Hu et al. (2008), using the *R* statistical software program StalAge (Scholz and Hoffmann, 2011) which are shown in Table 2. ^{14}C results are shown in Table 2 as conventional radiocarbon ages (Stuiver and Polach, 1977). Uncertainties are shown at 1σ and include contributions from background corrections, normalization to standards, as well as counting statistics.

3. Results

The record spanning 0.5–9.6 ka is plotted in uncalibrated ^{14}C years with IntCal13 in Fig. 2. The HS4 data shows reasonably constant offset from the IntCal13 record, but exhibits some interesting non-random structure including, most prominently, a sharp decrease in ^{14}C age before 9.2 ka (250 cm stalagmite depth) that is not seen in IntCal13. This sharp decrease in DCP before 9.2 ka, occurs concurrently with an increase in Mg/Ca, $\delta^{18}O$, $\delta^{13}C$ and ^{238}U (Supplementary Fig. 1) and is suggestive of mineralogical alteration of this lowest section of HS4 (see Supplementary Discussion). Because of this anomalous shift in speleothem geochemistry, measurements below 250 cm were not included in the calculation of the average DCP for the whole Holocene record. The mean DCP and standard deviation were calculated from the difference between each HS4 ^{14}C measurement and equivalent IntCal13 points, giving a mean DCP of $10.3 \pm 1.5\%$ (DCP correction of 875 ± 130 ^{14}C years). HS4 DCP is higher than Hulu Cave H82's DCP of $5.4 \pm 0.7\%$ (Southon et al., 2012), but significantly lower and less variable than the DCP of both of the speleothem records from the Bahamas (GB-89-25-3 = $22.7 \pm 5.9\%$, GB-89-24-1 = $16.5 \pm 4.7\%$) (Beck et al., 2001; Hoffmann et al., 2010)

Table 2
StalAge age model and radiocarbon measurements.

UCI-AMS #	Distance from top (cm)	StalAge model (yrs BP)	StalAge 1σ error	Fraction Modern	$\Delta^{14}C$ (‰)	^{14}C age (yrs BP)	^{14}C age DCF corrected (yrs BP)	DCP (%)
93 902	24.65	556	58	0.8394 ± 0.0012	−102.2 ± 1.2	1405 ± 15	530 ± 131	9.74 ± 0.66
77 412	28.5	651	49	0.8182 ± 0.0011	−114.8 ± 1.1	1610 ± 15	735 ± 131	11.37 ± 0.56
93 903	33	762	47	0.8043 ± 0.0016	−118.1 ± 1.6	1750 ± 20	875 ± 132	10.48 ± 0.56
77 413	43	985	94	0.7908 ± 0.0012	−109.2 ± 1.2	1885 ± 15	1010 ± 131	9.19 ± 1.05
93 904	48.25	1113	50	0.7740 ± 0.0011	−114.4 ± 1.1	2060 ± 15	1185 ± 131	10.26 ± 0.58
77 414	52.85	1253	25	0.7696 ± 0.0011	−104.5 ± 1.1	2105 ± 15	1230 ± 131	9.86 ± 0.34
77 415	59	1456	45	0.7324 ± 0.0011	−126.5 ± 1.1	2500 ± 15	1625 ± 131	10.75 ± 0.52
93 905	63.25	1634	48	0.7258 ± 0.0019	−115.5 ± 1.9	2575 ± 25	1700 ± 132	9.73 ± 0.60
77 416	67	1779	39	0.7127 ± 0.0012	−116.2 ± 1.2	2720 ± 15	1845 ± 131	10.48 ± 0.48
77 417	73	2004	27	0.7046 ± 0.0010	−102.2 ± 1.0	2815 ± 15	1940 ± 131	8.82 ± 0.35
77 418	78.6	2211	17	0.6844 ± 0.0010	−105.8 ± 1.0	3045 ± 15	2170 ± 131	9.61 ± 0.29
93 906	83.4	2382	23	0.6836 ± 0.0009	−88.1 ± 0.9	3055 ± 15	2180 ± 131	7.49 ± 0.33
77 421	85.25	2447	24	0.6781 ± 0.0010	−88.3 ± 1.0	3120 ± 15	2245 ± 131	8.32 ± 0.33
77 422	90.6	2633	21	0.6532 ± 0.0011	−101.7 ± 1.1	3420 ± 15	2545 ± 131	10.91 ± 0.31
93 907	95.45	2799	31	0.6375 ± 0.0009	−105.7 ± 0.9	3615 ± 15	2740 ± 131	10.44 ± 0.39
77 423	99.9	2927	35	0.6287 ± 0.0009	−104.3 ± 0.9	3730 ± 15	2855 ± 131	10.69 ± 0.43
93 908	104.5	3077	23	0.6300 ± 0.0023	−85.9 ± 2.3	3710 ± 30	2835 ± 133	9.29 ± 0.45
77 424	109	3225	27	0.6242 ± 0.0010	−78.0 ± 1.0	3785 ± 15	2910 ± 131	9.08 ± 0.37
93 909	111.7	3315	81	0.6081 ± 0.0010	−92.0 ± 1.0	3995 ± 15	3120 ± 131	11.18 ± 0.90
77 425	115	3446	178	0.5973 ± 0.0009	−93.8 ± 0.9	4140 ± 15	3265 ± 131	10.83 ± 1.93
93 910	118.35	3754	152	0.5917 ± 0.0009	−68.2 ± 0.9	4215 ± 15	3340 ± 131	8.72 ± 1.69
77 426	121.7	3931	26	0.5798 ± 0.0009	−67.2 ± 0.9	4380 ± 15	3505 ± 131	8.83 ± 0.36
77 427	131.5	4195	11	0.5568 ± 0.0010	−75.1 ± 1.0	4705 ± 15	3830 ± 131	10.36 ± 0.23
77 428	141.75	4480	34	0.5513 ± 0.0011	−52.1 ± 1.1	4785 ± 20	3910 ± 132	9.14 ± 0.44
93 913	145.85	4632	54	0.5353 ± 0.0009	−62.5 ± 0.9	5020 ± 15	4145 ± 131	10.38 ± 0.62
93 914	149.8	4817	57	0.5361 ± 0.0008	−39.9 ± 0.8	5010 ± 15	4135 ± 131	9.88 ± 0.65
77 429	154	4989	23	0.5201 ± 0.0009	−49.0 ± 0.9	5250 ± 15	4375 ± 131	9.70 ± 0.33
77 430	166	5456	29	0.4915 ± 0.0014	−49.1 ± 1.4	5705 ± 25	4830 ± 132	11.90 ± 0.41
93 915	169.1	5629	37	0.4772 ± 0.0008	−57.2 ± 0.8	5945 ± 15	5070 ± 131	12.10 ± 0.44
93 916	172.8	5894	91	0.4616 ± 0.0008	−58.2 ± 0.8	6210 ± 15	5335 ± 131	13.05 ± 0.98
77 433	176.7	6162	31	0.4443 ± 0.0008	−63.7 ± 0.8	6515 ± 15	5640 ± 131	14.14 ± 0.39
93 917	179	6384	92	0.4318 ± 0.0007	−65.3 ± 0.7	6745 ± 15	5870 ± 131	13.70 ± 0.98
93 918	181.15	6560	63	0.4329 ± 0.0007	−42.7 ± 0.7	6725 ± 15	5850 ± 131	11.28 ± 0.71
77 434	183.6	6634	36	0.4270 ± 0.0008	−47.3 ± 0.8	6835 ± 15	5960 ± 131	12.19 ± 0.44
77 464	193.25	6911	23	0.4198 ± 0.0010	−31.4 ± 1.0	6970 ± 20	6095 ± 132	10.78 ± 0.36
77 470	200.5	7134	75	0.4062 ± 0.0010	−37.4 ± 1.0	7240 ± 20	6365 ± 132	12.80 ± 0.83
77 435	208.1	7365	61	0.4055 ± 0.0007	−11.8 ± 0.7	7250 ± 15	6375 ± 131	9.85 ± 0.71
77 471	212.2	7490	68	0.4011 ± 0.0010	−7.6 ± 1.0	7340 ± 25	6465 ± 132	8.78 ± 0.81
77 465	216.7	7629	59	0.3914 ± 0.0009	−15.1 ± 0.9	7535 ± 20	6660 ± 132	8.83 ± 0.71
77 472	222	7783	95	0.3760 ± 0.0010	−36.0 ± 1.0	7860 ± 25	6985 ± 132	10.87 ± 1.07
77 466	228	7951	33	0.3696 ± 0.0009	−33.0 ± 0.9	7995 ± 25	7120 ± 132	10.45 ± 0.46
93 919	230.6	8050	20	0.3709 ± 0.0006	−17.9 ± 0.6	7965 ± 15	7090 ± 131	8.22 ± 0.39
94 750	232.05	8123	26	0.3668 ± 0.0012	−20.1 ± 1.2	8055 ± 30	7180 ± 133	9.28 ± 0.45
94 751	232.2	8131	26	0.3719 ± 0.0016	−5.5 ± 1.6	7945 ± 35	7070 ± 135	7.97 ± 0.45
93 920	232.25	8134	27	0.3624 ± 0.0008	−30.5 ± 0.8	8155 ± 20	7280 ± 132	10.23 ± 0.40
94 752	232.3	8137	27	0.3663 ± 0.0012	−19.9 ± 1.2	8070 ± 30	7195 ± 133	9.25 ± 0.53
94 753	232.35	8140	27	0.3692 ± 0.0009	−11.9 ± 0.9	8005 ± 20	7130 ± 132	8.62 ± 0.45
94 754	232.45	8145	28	0.3680 ± 0.0009	−14.3 ± 0.9	8030 ± 20	7155 ± 132	9.00 ± 0.45
94 755	232.55	8150	28	0.3642 ± 0.0016	−23.7 ± 1.6	8115 ± 35	7240 ± 135	9.91 ± 0.45
94 756	232.65	8156	28	0.3627 ± 0.0015	−27.2 ± 1.5	8145 ± 35	7270 ± 135	10.16 ± 0.45
94 757	232.75	8161	29	0.3651 ± 0.0009	−20.2 ± 0.9	8095 ± 20	7220 ± 132	9.44 ± 0.60
94 758	232.85	8167	29	0.3669 ± 0.0009	−14.6 ± 0.9	8055 ± 20	7180 ± 132	8.80 ± 0.48
94 759	232.95	8172	29	0.3686 ± 0.0009	−9.4 ± 0.9	8015 ± 25	7140 ± 132	8.23 ± 0.45
94 760	233.05	8178	30	0.3684 ± 0.0008	−9.3 ± 0.8	8020 ± 20	7145 ± 132	7.91 ± 0.46
94 761	233.15	8183	30	0.3689 ± 0.0008	−7.4 ± 0.8	8010 ± 20	7135 ± 132	7.59 ± 0.46
94 762	233.25	8189	30	0.3654 ± 0.0008	−16.2 ± 0.8	8090 ± 20	7215 ± 132	8.31 ± 0.46
94 763	233.35	8194	30	0.3659 ± 0.0009	−14.2 ± 0.9	8075 ± 25	7200 ± 132	8.09 ± 0.48
94 750	233.45	8200	30	0.3667 ± 0.0008	−11.3 ± 0.8	8060 ± 20	7185 ± 132	7.76 ± 0.45
94 751	233.55	8205	30	0.3652 ± 0.0012	−14.6 ± 1.2	8090 ± 30	7215 ± 133	8.01 ± 0.46
94 752	233.65	8211	30	0.3638 ± 0.0009	−17.8 ± 0.9	8125 ± 20	7250 ± 132	8.27 ± 0.70
94 753	233.75	8217	30	0.3638 ± 0.0016	−17.1 ± 1.6	8125 ± 40	7250 ± 136	8.17 ± 0.46
94 754	233.85	8222	30	0.3613 ± 0.0009	−23.3 ± 0.9	8180 ± 20	7305 ± 132	8.75 ± 0.46
77 473	233.9	8225	30	0.3548 ± 0.0009	−40.3 ± 0.9	8325 ± 20	7450 ± 132	10.35 ± 0.44
94 764	233.95	8228	30	0.3584 ± 0.0009	−30.5 ± 0.9	8245 ± 25	7370 ± 132	9.50 ± 0.45
94 765	234.05	8234	30	0.3572 ± 0.0008	−33.0 ± 0.8	8270 ± 20	7395 ± 132	9.80 ± 0.44
94 766	234.15	8239	30	0.3549 ± 0.0008	−38.5 ± 0.8	8320 ± 20	7445 ± 132	10.41 ± 0.44
94 767	234.25	8245	29	0.3590 ± 0.0008	−26.8 ± 0.8	8230 ± 20	7355 ± 132	9.44 ± 0.44
94 768	234.35	8251	29	0.3598 ± 0.0008	−23.8 ± 0.8	8210 ± 20	7335 ± 132	9.21 ± 0.45
94 769	234.45	8257	29	0.3581 ± 0.0009	−27.8 ± 0.9	8250 ± 20	7375 ± 132	9.59 ± 0.43
94 770	234.55	8263	29	0.3589 ± 0.0009	−24.9 ± 0.9	8230 ± 20	7355 ± 132	9.68 ± 0.42
94 771	234.65	8269	29	0.3588 ± 0.0010	−24.3 ± 1.0	8235 ± 25	7360 ± 132	9.77 ± 0.43
94 772	234.75	8275	29	0.3565 ± 0.0009	−30.1 ± 0.9	8285 ± 20	7410 ± 132	10.35 ± 0.49
94 773	234.85	8281	29	0.3559 ± 0.0009	−30.9 ± 0.9	8300 ± 20	7425 ± 132	10.40 ± 0.42

Table 2 (*Continued*)

UCI-AMS #	Distance from top (cm)	StalAge model (yrs BP)	StalAge 1σ error	Fraction Modern	$\Delta^{14}C$ (‰)	^{14}C age (yrs BP)	^{14}C age DCF corrected (yrs BP)	DCP (%)
94 774	234.95	8288	29	0.3582 ± 0.0012	−23.9 ± 1.2	8250 ± 30	7375 ± 133	9.78 ± 0.42
94 775	236.2	8371	29	0.3448 ± 0.0006	−50.8 ± 0.6	8555 ± 15	7680 ± 131	12.03 ± 0.38
94 776	237.7	8472	27	0.3406 ± 0.0035	−50.9 ± 3.5	8650 ± 90	7775 ± 158	11.13 ± 0.98
94 777	239.85	8609	33	0.3363 ± 0.0008	−47.1 ± 0.8	8755 ± 20	7880 ± 132	10.59 ± 0.46
94 778	242.3	8765	25	0.3353 ± 0.0006	−31.9 ± 0.6	8780 ± 15	7905 ± 131	9.98 ± 0.36
94 779	244.85	8927	16	0.3249 ± 0.0007	−43.5 ± 0.7	9030 ± 20	8155 ± 132	12.52 ± 0.32
77 468	247.75	9110	18	0.3276 ± 0.0008	−13.7 ± 0.8	8965 ± 20	8090 ± 132	9.45 ± 0.35
93 926	249.9	9246	21	0.3261 ± 0.0006	−2.1 ± 0.6	9000 ± 20	8125 ± 132	9.22 ± 0.40
93 927	252.35	9402	23	0.3379 ± 0.0008	53.8 ± 0.8	8715 ± 20	7840 ± 132	4.78 ± 0.41
77 469	254.05	9509	26	0.3307 ± 0.0008	44.7 ± 0.8	8890 ± 25	8015 ± 132	4.89 ± 0.43
93 928	255.4	9595	28	0.3318 ± 0.0036	58.9 ± 3.6	8860 ± 90	7985 ± 158	2.36 ± 1.13

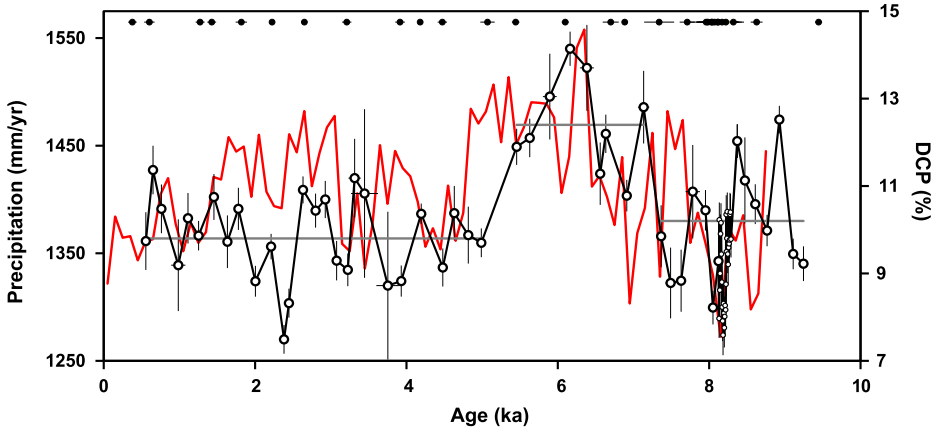

Fig. 3. Comparison of HS4 DCP (black) and precipitation at HS4 based on the $\Delta\delta^{18}O$ record from Hu et al. (2008) (red). $\Delta\delta^{18}O$ has been recalculated using HS4 on the StalAge model presented in this text. Grey bars show the means of the regimes identified with the sequential t-test method (Rodionov, 2004). U–Th dates are shown at the top of the figure. (For interpretation of the references to color in this figure legend, the reader is referred to the web version of this article.)

To assess whether non-random variability exists in the HS4 DCP record, a runs test utilizing the Matlab 'runstest' function was conducted, which rejected the null hypothesis (H_o) that the DCP variability is entirely random ($p < 0.0001$). Even if the clearly anomalous data prior to 9.2 ka is excluded, H_o can be rejected at the 90% significance level ($p = 0.0982$), suggesting that there is likely some non-random structure to the DCP residuals during other parts of the Holocene that may reflect minor influence of climate or other factors on speleothem DCP. To objectively identify periods of distinct DCP, a sequential t-test method (Rodionov, 2004; cut-off length = 10, $\alpha = 0.05$) was applied to identify statistically significant shifts between one or more DCP regimes. To avoid bias from the dense sampling around the 8.2 ka event, only the low-resolution HS4 DCP data was included in the analysis. Results show four distinct regimes: 0.556–4.989 ka (mean DCP = 9.8%), 5.456–7.134 ka (mean DCP = 12.4%), 7.365–9.246 ka (mean DCP = 10.2%), and 9.402–9.09 ka (mean DCP = 4.0%). The 8.2 ka event is characterized by decreased DCP values, with a minimum of 7.6% but this event is not recognized by the sequential *t*-test method, even when the high-resolution data is included in the analysis. Furthermore, *z*-scores were calculated for each DCP point. During the mid-Holocene period of elevated DCP, the probability of observing the two highest values, $z = 2.52$ and 2.28, is only 0.0058 and 0.0113 respectively, while during the 8.2 event, the probability of observing the lowest DCP value observed is 0.1170. Together, these results suggest that the elevated DCP observed during the mid-Holocene, from ~5.5 to 7.1 ka, is unlikely to represent random chance and instead may reflect a climatically driven shift in speleothem DCP. The observed DCP decrease during the 8.2 ka event, while it may also reflect a climatically driven shift, is less clear than the mid-Holocene shift.

The rapid decrease in DCP from 10.9% to 7.5% between 2.6–2.4 ka BP lags a peak at 2.7 ka in atmospheric ^{14}C caused by the Homeric Solar Minimum, and is therefore most likely an artifact of the fact that speleothem carbon is not directly sourced from atmospheric CO_2, but from soil CO_2. As was highlighted in Fohlmeister et al. (2011a) because of the contribution of old SOM to soil CO_2, centennial scale events in atmospheric ^{14}C, like solar events, will be smoothed in speleothem calcite and create apparent DCP excursions which are caused by comparing a smoothed record (the speleothem) with a higher resolution record (IntCal13).

4. Discussion

4.1. Climatic influences on DCP during the mid-Holocene

Paleoclimate records indicate that the mid-Holocene was wetter and warmer in central China, suggesting that the increase in DCP seen in HS4 during the mid-Holocene was climatically or hydrologically driven. Through comparison of the $\delta^{18}O$ record from Heshang Cave with a similar record from speleothem DA from Dongge Cave (25°17′N, 108°5′E, 680 m asl) (Wang et al., 2005), 600 km SW and along the same moisture trajectory as Heshang Cave, Hu et al. (2008) showed that annual rainfall in Southwest China was higher than modern values between 8.2 and 3.0 ka, peaking at 8% above the modern value between 6.4 and 5 ka. The period of increased rainfall between 6.4 and 5 ka represents the period of highest rainfall during the Holocene, indicating that the peak in DCP in this interval could be driven by increased precipitation and/or soil moisture (Fig. 3). Several modeling studies have confirmed the presence of a strengthened EASM during this interval. The Paleoclimate Modeling Intercomparison Project (PMIP) reported the results of 18 models that

showed that amplification of the northern hemispheric seasonal cycle of insolation during the mid-Holocene, specifically at 6 ka, caused a northward shift in monsoon precipitation (Joussaume et al., 1999). A well-dated peat core from Dajiuhu Lake located 125 km north of Heshang Cave (at 31.49°N, 109.99°E, 1760 m), has been studied extensively using a variety of paleoclimate proxies including pollen (Zhu et al., 2006, 2010; Chen et al., 2008; Zhao and Chen, 2010), minerogenic matter (Zhu et al., 2010), total organic carbon (Ma et al., 2008), and degree of humification (Ma et al., 2009). All proxies from the Dajiuhu peat core show the same general trend of gradually increasing summer monsoon strength from the Late-glacial interval to 6 ka, with interruptions at the Younger Dryas and 8.2 ka event. All proxies show the wettest, warmest, most stable values occurring between ~4.5–7.0, with an abrupt shift to drier and colder conditions occurring ~4.2–4.5 ka, and pollen records indicating peak monsoon strength at 6 ka (Zhu et al., 2010). The good agreement between the interval of highest monsoon intensity in the Holocene as shown by the paleoclimate records and the period of increased DCP in HS4 suggests a relationship between rainfall amount and DCP.

The change in DCP due to changing rainfall amount could be caused by accelerating SOM decomposition rates, and therefore increasing mean age of soil gas CO_2, and/or changing open/closed system dissolution. The mean DCP correction during the mid-Holocene period of increased DCP is 1065 years, while the mean DCP corrections during the early-Holocene and late-Holocene are 845 years and 830 years respectively. If the mid-Holocene increase in DCP was entirely due to increasing decomposition rate of old SOM, and therefore increasing soil CO_2 age, the mean age of soil CO_2 would have had to increase by ~220 years for a period of 1.6 ka during the mid-Holocene. If we make the assumption that SOM was at steady state during the early-Holocene, and no longer at equilibrium during the mid-Holocene when decomposition of the old SOM pools was greatly accelerated causing the mean age of soil CO_2 to increase by 220 years, we can do a simple mass balance calculation to estimate if it is possible for the mid-Holocene increase in DCP to be caused predominately by an increase in the mean age of soil CO_2.

SOM in tropical sites that have been studied using ^{14}C, which may not be analogous to SOM in karst sites, show that ~20% of the SOM has a turnover time of <10 years, 60% has a turnover time on the order of decades, and 20% has a turnover time of >6000 (Trumbore, 2000). For simplicity, in our mass balance calculations we consider only two SOM pools, an annual pool, and a millennial pool, and assume that the mass of the contribution from the annual pool stays constant between the steady state and the accelerated decomposition modes. Decomposition of a millennial pool with a mean age of >5000 years would initially have to be occurring roughly 650 times faster than at steady state if the pool accounted for 25% of the SOM, and 215 times faster if the pool accounted for 50% of the SOM to achieve the 220 year increase in mean age of soil CO_2, and either case would result in the complete consumption of the millennial pool on a timescale on the order of decades – much less than necessary to explain the 1.6 ka long period of increased DCP seen in HS4 at the mid-Holocene.

Moreover, barring a major disturbance event like tilling or fire, which would have effects that are much shorter in duration than the mid-Holocene period of DCP increase, the decomposition rates of old SOM required for increasing soil CO_2 age to be the primary cause of the increase in DCP seen at the mid-Holocene in HS4 are difficult to explain physically. The Q10 of SOM decomposition, the increase in reaction rates given a 10 °C increase in temperature, is generally thought to be about 2 (Davidson and Janssens, 2006), ruling out warming as the cause of the increase in SOM decomposition rates necessary to increase the mean age of soil CO_2 by 220 years. The increase in precipitation known to have occurred during the mid-Holocene at Heshang Cave would be expected to cause a decrease in SOM decomposition because increased soil moisture would limit oxygen diffusion in the soil, shifting decomposition towards a more anaerobic mode which is a slower process (Davidson and Janssens, 2006). Additionally, observations of soil $^{14}CO_2$ show that soil CO_2 has a mean age of ~1 year in tropical sites, ~3 years in temperate sites, and ~16 years in boreal sites (Trumbore, 2000), suggesting that soil CO_2 mean ages on the order of hundreds of years are unlikely in a sub-tropical site like Heshang Cave.

There has been some effort to understand how changing SOM decomposition affects speleothem DCP (e.g. Genty and Massault, 1999; Fohlmeister et al., 2010, 2011a, 2011b; Griffiths et al., 2012, Rudzka et al., 2011; Rudzka-Phillips et al., 2013) most often using a simple three-box soil carbon model and the shape of the atmospheric ^{14}C bomb peak in modern speleothems to estimate the relative size and turnover times of three SOM pools. The models employed in these studies require that the soil CO_2 equilibrating with the soil water DIC have mean ages ranging from ~40 to 500 years during the twentieth century (Rudzka-Phillips et al., 2013), which appears to be at odds with the observations of soil CO_2. This discrepancy between the age distribution of soil carbon incorporated in DIC required by the shape of the bomb peak observed in speleothems, and the observations of soil CO_2 ages is a critical point in our understanding of the role of dead carbon incorporation in speleothems. The discrepancy suggests that it is very likely that processes in soils above karsts are unlike those in sites where soil CO_2 age has been studied to date, therefore limiting our ability to interpret the role of changing age of soil $^{14}CO_2$ on DCP in speleothems.

Given observations of the mean age of soil CO_2 observed in tropical sites (Trumbore, 2000), we tend to favor the explanation that changes in the offset between speleothem calcite and contemporaneous atmospheric ^{14}C of centennial magnitude in observed in the mid-Holocene in HS4 were driven by an increasing proportion of the dripwater DIC derived from the bedrock – that is a more closed system dissolution regime. A similar relationship between rainfall amount and DCP as is observed in HS4 was observed in a record based on an Indonesian speleothem, LR06-B1 from Liang Luar Cave (8°32′N, 120°26′W) (Griffiths et al., 2012). Griffiths et al. (2012) hypothesized that increased precipitation at the cave site would increase saturation of the voids in the soil zone, thereby limiting exchange between soil gas and soil moisture. Lower CO_2 diffusion in the soil zone due to soil saturation would shift dissolution to a more closed system, increasing speleothem DCP by increasing the relative proportion of carbon sourced from the radiocarbon-free limestone host rock. Conversely, periods of decreased rainfall should lead to lower DCP as soil would be less saturated, allowing for more CO_2 diffusion, and would lead to more open system dissolution. The increased DCP observed in HS4 during the mid-Holocene (~5.5–7.1 ka) is consistent with this mechanism and indicates that increases in precipitation may in fact lead to more closed system dissolution and a higher DCP.

4.2. Climatic influences on DCP during the 8.2 ka event

Hu et al. (2008) showed that the most pronounced dry event at Heshang Cave occurred at 8.2 ka, when rainfall was ~7% lower than present. This interval was identified by Liu et al. (2013) as having synchronous onset and similar duration to the 8.2 ka event seen in the Greenland ice core record. HS4 $\delta^{18}O$, Mg/Ca, and layer thickness data demonstrate that the 8.2 ka event at Heshang Cave was characterized by an abrupt decrease in precipitation that lasted for 150 years. To investigate the effect of abrupt precipitation decreases on DCP, the 8.2 ka interval was sampled for ^{14}C at high resolution. These high-resolution ^{14}C measurements show a rapid decrease in DCP to a minimum of 7.6% (Fig. 4),

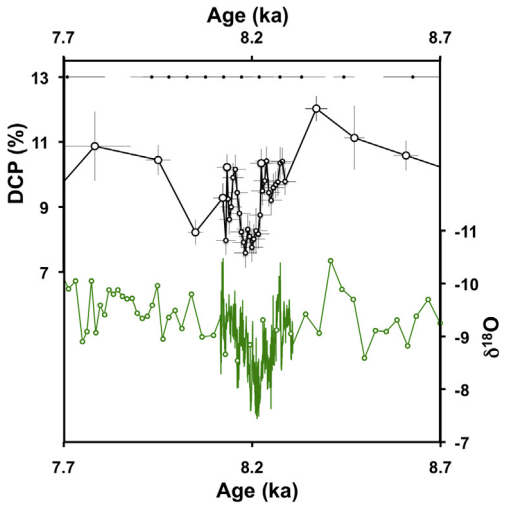

Fig. 4. Plot of DCP and $\delta^{18}O$ in the interval defined by the 8.2 ka event. Top panel shows high-resolution measurements of DCP at 8.2 ka event as small open circles and lower resolution measurements as larger open circles. Bottom panel shows high-resolution $\delta^{18}O$ measurements covering the 8.2 ka event (Liu et al., 2013) without markers and lower resolution $\delta^{18}O$ measurements in the interval (Hu et al., 2008) shown with open circles. Both $\delta^{18}O$ records are plotted on the StalAge age model presented in this manuscript. U–Th ages defining this interval, including the 10 Bayesian OxCal corrected ages, are shown at the top of the figure.

but the interval is not significantly different than the proceeding early Holocene DCP values as demonstrated by a sequential t-test method (Rodionov, 2004). If the relationship between rainfall amount and DCP described by Griffiths et al. (2012) controls DCP in HS4, we might expect a more pronounced drop in DCP at the 8.2 ka event. Under this mechanism, decreases in DCP during periods of lower rainfall are driven by more open system dissolution because of increased exchange between soil CO_2 and DIC in soil moisture relative to the exchange that would occur in a saturated soil zone. A possible explanation of the muted DCP response to the 8.2 ka dry event at Heshang Cave is that the relationship between closed-vs-open system dissolution and rainfall amount may be non-linear. A completely closed system dissolution regime would result in DCP of 50%, indicating that even during the mid-Holocene when DCP reached a high of 14.1%, carbonate dissolution took place in a largely open system. There is likely a limit to how much the lack of saturation of voids in the soil zone increases exchange between soil CO_2 and soil moisture, i.e. once soil reaches a specific level of dryness, the degree of open-system dissolution will be less sensitive to further decreases in soil moisture. Moreover, even in a completely open system, where all speleothem carbon is derived from soil CO_2, there will be some contribution of ^{14}C-depleted carbon from aged SOM, putting a lower limit on speleothem DCP. The lack of a significant decrease in DCP in HS4 at the 8.2 ka event suggests that DCP in speleothems formed in relatively open system regimes, i.e. speleothems with low average DCP, may be less affected by dry events than by wet events.

Consistent with this hypothesis, DCP is remarkably stable in Hulu Cave speleothem H82 throughout the Younger Dryas (YD) climate event, which was likely a period of reduced EASM intensity (Wang et al., 2001; Yancheva et al., 2007). The Bahamas speleothem GB-89-24-1 is also stable over the Younger Dryas interval, though GB-89-25-3, which has a much higher average DCP, shows large fluctuations in DCP at the YD suggesting that climate did have an effect on DCP in some speleothems in the region during the YD interval. Rudzka et al. (2011) produced records of DCP over the YD interval in three stalagmites: So-1 from Sofular Cave in northwestern Turkey (41°25′N, 31°56′E), stalagmite Candela from El Pindal Cave in northern Spain (43°23′N, 4°30′W), and stalagmite GAR-01 from La Garma Cave in northern Spain (43°24′N, 3°39′W) which also show muted responses to the YD in DCP. There is a decrease of $3.24 \pm 2.27\%$ (1σ) in DCP in the Turkish speleothem, So-1, between the two measurements bracketing the Bølling–Allerød/YD transition (from $9.58 \pm 1.87\%$ at 13.1 ka to $6.34 \pm 1.29\%$ at 12.8 ka), but DCP rebounds to pre-YD values by the next measurement at 12.4 ka. The two speleothems from Northern Spain, Candela and GAR-01, are separated by only 70 km but display very different responses to the YD climate event. Candela shows a largely stable DCP over the YD interval, with some indication of a slight increasing trend in DCP. GAR-01 shows a decrease in DCP of $4.43 \pm 1.77\%$ (pre-YD maximum of $6.13 \pm 1.15\%$ to a mean of $1.7 \pm 1.72\%$) at the onset of the YD, but DCP rebounds to $5.42 \pm 0.92\%$ at 12.2 ka and drops back to a mean of $1.93 \pm 1.34\%$ for the remainder of the YD interval. Given the high uncertainty, low resolution, and lack of knowledge of what the range of variability is in DCP in GAR-01 over stable climate intervals, it is difficult to assess whether the decreases in GAR-01 are significant. We interpret HS4, H82, GB-89-24-1, So-1 and Candela as speleothems with low average DCP without pronounced drops in DCP during dry events, lending support to the hypothesis that DCP in some speleothems with low DCP may be somewhat less sensitive to decreases in rainfall amount. However, many of these records are limited in duration and do not span periods of precipitation increase so it is difficult to discern with certainty whether this asymmetric response of DCP to rainfall amount observed in Heshang Cave exists in other speleothems, and more speleothem records covering both stable climate intervals and abrupt climate transitions need to be investigated to verify this hypothesis.

5. Conclusions

This new high-resolution record of ^{14}C from speleothem HS4 from Heshang Cave, China, contributes to the developing understanding of the controls on variability of dead carbon incorporation in speleothems, which is critically important to our ability to use speleothems as records of atmospheric ^{14}C. This record shows evidence of climatically controlled variation in DCP, with an increase in DCP during the warmer and wetter mid-Holocene interval, and a smaller shift towards lower DCP during the 8.2 ka dry event. We suggest that the increase in precipitation during the mid-Holocene caused increased soil moisture, which limited diffusion of soil CO_2 and equilibration between soil moisture and soil CO_2, therefore shifting carbonate dissolution towards a more closed system regime and increasing DCP. The lower amplitude change in DCP during the very dry 8.2 ka event suggests that there may be an asymmetric response of speleothem DCP to rainfall amount. Development of other speleothem ^{14}C records that span both wet and dry events is necessary to confirm this mechanism, and continue to develop understanding of the controls on variability in dead carbon incorporation in speleothems.

Acknowledgements

We would like to thank Yuhui Liu and Gideon Henderson for information regarding the 8.2 ka event in HS4, Silvia Frisia for assistance with thin section interpretation, and David Richards, and two anonymous reviewers for their suggestions that greatly improved this manuscript. This research was supported by NSF AGS-0903101 to KRJ, an NSF EAPSI grant number 1107922 to ALN, and NSFC 41072262 to HCY.

Appendix A. Supplementary material

Supplementary material related to this article can be found online at http://dx.doi.org/10.1016/j.epsl.2014.03.015.

References

Bard, E., 1998. Geochemical and geophysical implications of the radiocarbon calibration. Geochim. Cosmochim. Acta 62 (12), 2025–2038.

Beck, J.W., Richards, D.A., Edwards, R.L., Silverman, B.W., Smart, P.L., Donahue, D.J., Hererra-Osterheld, S., Burr, G.S., Calsoyas, L., Jull, A.J., Biddulph, D., 2001. Extremely large variations of atmospheric ^{14}C concentration during the last glacial period. Science 292 (5526), 2453–2458. http://dx.doi.org/10.1126/science.1056649.

Broecker, W., Barker, S., 2007. A 190‰ drop in atmosphere's $\Delta^{14}C$ during the "Mystery Interval" (17.5 to 14.5 kyr). Earth Planet. Sci. Lett. 256 (1–2), 90–99. http://dx.doi.org/10.1016/j.epsl.2007.01.015.

Bronk Ramsey, C., 2008. Deposition models for chronological records. Quat. Sci. Rev. 27 (1–2), 42–60. http://dx.doi.org/10.1016/j.quascirev.2007.01.019.

Bronk Ramsey, C., et al., 2012. A complete terrestrial radiocarbon record for 11.2 to 52.8 kyr B.P. Science 338 (6105), 370–374. http://dx.doi.org/10.1126/science.1226660.

Chen, X., Zhu, C., Ma, C., Fan, C., 2008. Sensitivity of pollen factors in the climate transfer function. Chin. Sci. Bull. 53 (S1), 50–57. http://dx.doi.org/10.1007/s11434-008-5002-y.

Davidson, E.A., Janssens, I.A., 2006. Temperature sensitivity of soil carbon decomposition and feedbacks to climate change. Nature 440 (7081), 165–173. http://dx.doi.org/10.1038/nature04514.

Dorale, J.A., Southon, J.R., Edwards, R.L., 2008. High-resolution radiocarbon calibration from 30–50 ka based on stalagmite ^{14}C and ^{230}Th ages. Geochim. Cosmochim. Acta 72 (12), A224.

Fairchild, I.J., Smith, C.L., Baker, A., Fuller, L., Spötl, C., Mattey, D., McDermott, F., 2006. Modification and preservation of environmental signals in speleothems. Earth-Sci. Rev. 75 (1–4), 105–153. http://dx.doi.org/10.1016/j.earscirev.2005.08.003.

Fohlmeister, J., Schröder-Ritzrau, A., Spötl, C., 2010. The influences of hydrology on the radiogenic and stable carbon isotope composition of cave drip water, Grotta Di Ernesto (Italy). Radiocarbon 52 (4), 1529–1544.

Fohlmeister, J., Scholz, D., Kromer, B., Mangini, a., 2011a. Modelling carbon isotopes of carbonates in cave drip water. Geochim. Cosmochim. Acta 75 (18), 5219–5228. http://dx.doi.org/10.1016/j.gca.2011.06.023.

Fohlmeister, J., Kromer, B., Mangini, A., 2011b. The influence of soil organic matter age spectrum on the reconstruction of atmospheric ^{14}C levels via stalagmites. Radiocarbon 53 (1).

Frisia, S., Borsato, A., 2010. Karst. In: Alonso-Zarza, A.M., Tanner, H.L. (Eds.), Carbonates in Continental Settings: Facies, Environments, and Processes. In: Dev. Sedimentol., vol. 61. Elsevier, pp. 269–318, Chapter 6.

Genty, D., Massault, M., 1997. Bomb ^{14}C recorded in laminated speleothems: calculations of dead carbon proportion. Radiocarbon 39 (1), 33–48.

Genty, D., Massault, M., 1999. Carbon transfer dynamics from bomb-^{14}C and $\delta^{13}C$ time series of a laminated stalagmite from SW France—modeling and comparison with other stalagmite records. Geochim. Cosmochim. Acta 63 (10), 1537–1548. http://dx.doi.org/10.1016/S0016-7037(99)00122-2.

Genty, D., Massault, M., Gilmour, M., Baker, A., Verheyden, S., Kepens, E., 1999. Calculation of past dead carbon proportion and variability by the comparison of AMS ^{14}C and TIMS U/Th ages on two Holocen stalagmites. Radiocarbon 41 (3), 251–270.

Gill, I., Olson, J.J., Hubbard, D.K., 1995. Corals, paleotemperature records, and the aragonite–calcite transformation. Geology 23 (4), 333.

Griffiths, M.L., Fohlmeister, J., Drysdale, R.N., Hua, Q., Johnson, K.R., Hellstrom, J.C., Gagan, M.K., Zhao, J.-X., 2012. Hydrological control of the dead carbon fraction in a Holocene tropical speleothem. Quat. Geochronol. 14, 81–93. http://dx.doi.org/10.1016/j.quageo.2012.04.001.

Hendy, C., 1971. The isotopic geochemistry of speleothems—I. The calculation of the effects of different modes of formation on the isotopic composition of speleothems and their applicability as palaeoclimatic indicators. Geochim. Cosmochim. Acta 35 (8), 801–824. http://dx.doi.org/10.1016/0016-7037(71)90127-X.

Hoffmann, D.L., Beck, J.W., Richards, D.A., Smart, P.L., Singarayer, J.S., Ketchmark, T., Hawkesworth, C.J., 2010. Towards radiocarbon calibration beyond 28 ka using speleothems from the Bahamas. Earth Planet. Sci. Lett. 289 (1–2), 1–10. http://dx.doi.org/10.1016/j.epsl.2009.10.004.

Hogg, A.G., et al., 2013. The New Zealand Kauri (Agathis Australis) research project: a radiocarbon dating intercomparison of younger dryas wood and implications for IntCal13. Radiocarbon 55 (2), 2035–2048.

Hu, C., Henderson, G.M., Huang, J., Xie, S., Sun, Y., Johnson, K.R., 2008. Quantification of Holocene Asian monsoon rainfall from spatially separated cave records. Earth Planet. Sci. Lett. 266 (3–4), 221–232. http://dx.doi.org/10.1016/j.epsl.2007.10.015.

Hua, Q., et al., 2009. Atmospheric ^{14}C variations derived from tree rings during the early Younger Dryas. Quat. Sci. Rev. 28 (25–26), 2982–2990. http://dx.doi.org/10.1016/j.quascirev.2009.08.013.

Hughen, K.A., Southon, J.R., Lehman, S.J., Overpeck, J.T., 2000. Synchronous radiocarbon and climate shifts during the last deglaciation. Science 290 (5498), 1951–1954. http://dx.doi.org/10.1126/science.290.5498.1951.

Johnson, K., Hu, C., Belshaw, N., Henderson, G., 2006. Seasonal trace-element and stable-isotope variations in a Chinese speleothem: The potential for high-resolution paleomonsoon reconstruction. Earth Planet. Sci. Lett. 244 (1–2), 394–407. http://dx.doi.org/10.1016/j.epsl.2006.01.064.

Joussaume, S., et al., 1999. Monsoon changes for 6000 years ago: Results of 18 simulations from the Paleoclimate Modeling Intercomparison Project (PMIP). Geophys. Res. Lett. 26 (7), 859–862. http://dx.doi.org/10.1029/1999GL900126.

Kitagawa, H., van der Plicht, J., 1998a. A 40,000-year varve chronology from Lake Suigetsu, Japan: Extension of the ^{14}C calibration curve. Radiocarbon 40 (1), 505–515.

Kitagawa, H., van der Plicht, J., 1998b. Atmospheric radiocarbon calibration to 45,000 yr B.P.: late glacial fluctuations and cosmogenic isotope production. Science 279 (5354), 1187–1190. http://dx.doi.org/10.1126/science.279.5354.1187.

Kitagawa, H., van der Plicht, J., 2000. Atmospheric radiocarbon calibration beyond 11,900 cal BP from Lake Suigetsu laminated sediments. Radiocarbon 42 (3), 369–380.

Kromer, B., Friedrich, M., Hughen, K.A.A., Kaiser, F., Remmele, S., Schaub, M., Talamo, S., 2004. Late Glacial ^{14}C ages from a floating, 1382-ring pine chronology. Radiocarbon 46 (3), 1203–1209.

Liu, Y.-H., Henderson, G.M., Hu, C.-Y., Mason, A.J., Charnley, N., Johnson, K.R., Xie, S.-C., 2013. Links between the East Asian monsoon and North Atlantic climate during the 8200 year event. Nat. Geosci. 6 (2), 117–120. http://dx.doi.org/10.1038/ngeo1708.

Ma, C., Zhu, C., Zheng, C., Wu, C., Guan, Y., Zhao, Z., Huang, L., Huang, R., 2008. High-resolution geochemistry records of climate changes since late-glacial from Dajiuhu peat in Shennongjia Mountains, Central China. Chin. Sci. Bull. 53 (S1), 28–41. http://dx.doi.org/10.1007/s11434-008-5007-6.

Ma, C., Zhu, C., Zheng, C., Yin, Q., Zhao, Z., 2009. Climate changes in East China since the Late-glacial inferred from high-resolution mountain peat humification records. Sci. China, Ser. D, Earth Sci. 52 (1), 118–131. http://dx.doi.org/10.1007/s11430-009-0003-5.

McDermott, F., Jackson, A.S., Mangini, A., Mattey, D.P., Frisia, S., 2008. ^{14}C variability in two late Holocene stalagmites and the implications for climate forcing mechanisms. Geochim. Cosmochim. Acta 72 (12), A612.

McManus, J.F., Francois, R., Gherardi, J.-M., Keigwin, L.D., Brown-Leger, S., 2004. Collapse and rapid resumption of Atlantic meridional circulation linked to deglacial climate changes. Nature 428 (6985), 834–837. http://dx.doi.org/10.1038/nature02494.

Morrill, C., Overpeck, J.T., Cole, J.E., 2003. A synthesis of abrupt changes in the Asian summer monsoon since the last deglaciation. Holocene 13 (4), 465–476. http://dx.doi.org/10.1191/0959683603hl639ft.

Muscheler, R., Kromer, B., Björck, S., Svensson, A., Friedrich, M., Kaiser, K.F., Southon, J., 2008. Tree rings and ice cores reveal ^{14}C calibration uncertainties during the Younger Dryas. Nat. Geosci. 1 (4), 263–267. http://dx.doi.org/10.1038/ngeo128.

Reimer, P., et al., 2013. IntCal13 and Marine13 radiocarbon age calibration curves 0–50,000 years cal BP. Radiocarbon 55 (4), 1869–1887.

Richards, D.A., Dorale, J.A., 2003. Uranium-series chronology and environmental applications of speleothems. In: Bourdon, B., Henderson, G.M., Lundstrom, C.C., Turner, S.P. (Eds.), Rev. Mineral. Geochem. 52 (1), 407–460. http://dx.doi.org/10.2113/0520407.

Rodionov, S.N., 2004. A sequential algorithm for testing climate regime shifts. Geophys. Res. Lett. 31 (9), L09204. http://dx.doi.org/10.1029/2004GL019448.

Rudzka, D., McDermott, F., Baldini, L.M., Fleitmann, D., Moreno, A., Stoll, H., 2011. The coupled $\delta^{13}C$-radiocarbon systematics of three Late Glacial/early Holocene speleothems insights into soil and cave processes at climatic transitions. Geochim. Cosmochim. Acta 75 (15), 4321–4339. http://dx.doi.org/10.1016/j.gca.2011.05.022.

Rudzka-Phillips, D., McDermott, F., Jackson, A., Fleitmann, D., 2013. Inverse modelling of the ^{14}C bomb pulse in stalagmites to constrain the dynamics of soil carbon cycling at selected European cave sites. Geochim. Cosmochim. Acta 112, 32–51. http://dx.doi.org/10.1016/j.gca.2013.02.032.

Scholz, D., Hoffmann, D.L., 2011. StalAge – An algorithm designed for construction of speleothem age models. Quat. Geochronol. 6 (3–4), 369–382. http://dx.doi.org/10.1016/j.quageo.2011.02.002.

Southon, J., Noronha, A.L., Cheng, H., Edwards, R.L., Wang, Y., 2012. A high-resolution record of atmospheric ^{14}C based on Hulu Cave speleothem H82. Quat. Sci. Rev. 33, 32–41. http://dx.doi.org/10.1016/j.quascirev.2011.11.022.

Staff, R.A., Bronk Ramsey, C., Nakagawa, T., 2010. A re-analysis of the Lake Suigetsu terrestrial radiocarbon calibration dataset. Nucl. Instrum. Methods Phys. Res., Sect. B, Beam Interact. Mater. Atoms 268 (7–8), 960–965. http://dx.doi.org/10.1016/j.nimb.2009.10.074.

Stuiver, M., Polach, H.A., 1977. Reporting of C-14 data. Radiocarbon 19 (3), 355–363.

Trumbore, S., 2000. Age of soil organic matter and soil respiration: radiocarbon constraints on belowground C dynamics. Ecol. Appl. 10 (2), 399–411.

Turney, C., Fifield, L., Palmer, J., 2007. Towards a radiocarbon calibration for oxygen isotope stage 3 using New Zealand Kauri (Agathis Australis). Radiocarbon 49 (2), 447–457.

Vellinga, M., Wood, R., 2002. Global climatic impacts of a collapse of the Atlantic thermohaline circulation. Clim. Change, 251–267. http://dx.doi.org/10.1023/A:1016168827653.

Wang, Y., Cheng, H., Edwards, R.L., He, Y., Kong, X., An, Z., Wu, J., Kelly, M.J., Dykoski, C.A., Li, X., 2005. The Holocene Asian monsoon: links to solar changes and North Atlantic climate. Science 308 (5723), 854–857. http://dx.doi.org/10.1126/science.1106296.

Wang, Y., Cheng, H., Edwards, R.L., Kong, X., Shao, X., Chen, S., Wu, J., Jiang, X., Wang, X., An, Z., 2008. Millennial- and orbital-scale changes in the East Asian monsoon over the past 224,000 years. Nature 451 (7182), 1090–1093. http://dx.doi.org/10.1038/nature06692.

Wang, Y.J., Cheng, H., Edwards, R.L., An, Z.S., Wu, J.Y., Shen, C.C., Dorale, J.A., 2001. A high-resolution absolute-dated late Pleistocene Monsoon record from Hulu Cave, China. Science 294 (5550), 2345–2348. http://dx.doi.org/10.1126/science.1064618.

Weyhenmeyer, C.E., Burns, S.J., Fleitmann, D., Kramers, J.D., Matter, A., Waber, H.N., Reimer, P.J., 2003. Changes in atmospheric ^{14}C between 55 and 42 ky BP recorded in a stalagmite from Socotra Island, Indian Ocean. In: Fall Meeting Supplement. EOS Trans. AGU 84 (46), Abstract PP32B-0289.

Yancheva, G., Nowaczyk, N.R., Mingram, J., Dulski, P., Schettler, G., Negendank, J.F.W., Liu, J., Sigman, D.M., Peterson, L.C., Haug, G.H., 2007. Influence of the intertropical convergence zone on the East Asian monsoon. Nature 445 (7123), 74–77. http://dx.doi.org/10.1038/nature05431.

Zhao, C., Chen, X., 2010. Climatological significance of Pollen factors revealed by pollen-climate response surface functions in Dajiuhu, Shennongjia. Acta Meteorol. Sin. 24 (6), 699–712.

Zhu, C., Ma, C., Zhang, W., Zheng, C., Tang, L., Lu, X., Liu, K., Chen, H., 2006. Pollen record from Dajiuhu basin of Shennongjia and environmental changes since 15.753 ka BP. Quat. Sci. 26 (5), 814–826.

Zhu, C., Ma, C., Yu, S.-Y., Tang, L., Zhang, W., Lu, X., 2010. A detailed pollen record of vegetation and climate changes in Central China during the past 16,000 years. Boreas 39 (1), 69–76. http://dx.doi.org/10.1111/j.1502-3885.2009.00098.x.